Biol. Cybern. 79, 139–150 (1998)

Biological
Cybernetics

Coordinated force production in multi-finger tasks: finger interaction and neural network modeling

Vladimir M. Zatsiorsky, Zong-Ming Li, Mark L. Latash

Biomechanics Laboratory, Department of Kinesiology, The Pennsylvania State University, University Park, PA 16802, USA

Received: 17 October 1997 / Accepted in revised form: 12 May 1998

Abstract During maximal voluntary contraction (MVC) with several fingers, the following three phenomena are observed: (1) the total force produced by all the involved fingers is shared among the fingers in a specific manner (*sharing*); (2) the force produced by a given finger in a multi-finger task is smaller than the force generated by this finger in a single-finger task (*force deficit*); (3) the fingers that are not required to produce any force by instruction are involuntary activated (*enslaving*). We studied involuntary force production by individual fingers (*enslaving effects*, EE) during tasks when (an)other finger(s) of the hand generated maximal voluntary pressing force in isometric conditions. The subjects ($n = 10$) were instructed to press as hard as possible on the force sensors with one, two, three and four fingers acting in parallel in all possible combinations. The EE were (A) large, the slave fingers always producing a force ranging from 10.9% to 54.7% of the maximal force produced by the finger in the single-finger task; (B) nearly symmetrical; (C) larger for the neighboring fingers; and (D) non-additive. In most cases, the EE from two or three fingers were smaller than the EE from at least one finger (this phenomenon was coined *occlusion*). The occlusion cannot be explained only by anatomical musculo-tendinous connections. Therefore, neural factors contribute substantially to the EE. A neural network model that accounts for all the three effects has been developed. The model consists of three layers: the input layer that models a central neural drive; the hidden layer modeling transformation of the central drive into an input signal to the muscles serving several fingers simultaneously (multi-digit muscles); and the output layer representing finger force output. The output of the hidden layer is set inversely proportional to the number of fingers involved. In addition, direct connections between the input and output layers represent signals to the hand muscles serving individual fingers (uni-digit muscles). The network was validated using three different training sets. Single digit muscles contributed from 25% to 50% of the total finger force. The master matrix and the enslaving matrix were computed; they characterize the ability of a given finger to enslave other fingers and its ability to be enslaved. Overall, the neural network modeling suggests that no direct correspondence exists between neural command to an individual finger and finger force. To produce a desired finger force, a command sent to an intended finger should be scaled in accordance with the commands sent to the other fingers.

Correspondence to: V.M. Zatsiorsky
(e-mail: vxz1@psu.edu,
Tel.: +1-814-8653445, Fax: +1-814-8652440)

1 Introduction

During maximal voluntary force production by several fingers acting in parallel, the total force is shared among involved fingers in a specific manner (*sharing*), while the force produced by a given finger in a multi-finger task is smaller than the force generated by this finger in a single-finger task (*force deficit*, Li et al. 1998a,b). *Force sharing* among individual fingers is a typical example of the motor redundancy problem: many different combinations of individual finger forces can achieve the same total force. This problem, also known as Bernstein's problem (Bernstein 1967), has been experimentally addressed at the level of individual muscles contributing to a joint torque (for reviews, see Crowninshield and Brand 1981b; Zatsiorsky and Prilutsky 1992; Latash 1996; Prilutsky et al. 1996) and individual joints contributing to a multi-joint motion (Rosenbaum et al. 1993). Previous studies have shown that the central nervous system (CNS) does not use all of the conceivable options for solving such problems. It prefers a single solution (a sharing pattern in finger force production tasks) and employs this solution for a range of total force values (Li et al. 1998a, b).

The prevailing approach in modeling the redundancy problem is based on an assumption that the CNS is using a certain optimization criterion – in the framework of such models the brain is replaced by a cost function.

Though various cost functions have been suggested and tried (Crowninshield et al. 1978; Herzog 1996; Crowninshield and Brand 1981a; Brand et al. 1986; Prilutsky and Zatsiorsky 1994), the majority of the employed cost functions fall in one group: they provide a minimal norm solution (Kuo 1994). A norm $N = (\sum x_i^n)^{1/n}$ where x_i is a performance variable (e.g. muscle force, force per unit of muscle cross-sectional area, the moment produced by a certain muscle, or the mechanical work produced at a joint) has been introduced and then minimized. However, the optimization approach can only account for the sharing phenomena and does not address other phenomena, such as force deficit.

The contribution of individual fingers to total force production is a convenient phenomenon for investigating the Bernstein problem. Finger forces can easily be measured (cf. with the muscle-tendon forces) and the sharing calculation is rudimentary – the total output/force is merely a sum of individual inputs/finger forces.

Force deficit among fingers (Ohstuki 1981) is similar to the well-known phenomenon of bilateral deficit (Schantz et al. 1989; Howard and Enoka 1991). In both cases the maximal force generated by an individual effector (finger, arm, leg) in a multi-effector task is less than the force in a single-effector task. In the multi-finger tasks the force deficit was explained by the *ceiling hypothesis*: the total neural drive to all the fingers is somehow limited and, as a result, the activation of a given finger reduces the drive to the other fingers (Li et al. 1998a,b).

With the present study we investigated effects that have been termed *enslaving effects*. Maximal isometric activation of some fingers is always accompanied by activity of the other fingers. When a subject is asked to press maximally with one, two, or three fingers, other fingers of the hand also produce a certain force. The explicitly involved fingers are addressed as *master fingers* while other force-producing fingers are termed *slave fingers*.

The goal of this study was twofold: first, to study interaction among the fingers and the enslaving effects during multi-finger force production; second, to develop and test a neural network model that accounts for all the three phenomena – sharing, force deficit, and enslaving.

2 Methods

2.1 Subjects

Ten right-handed university male students (weight 77.5 ± 8.5 kg, height 1.73 ± 0.04 m; hand length from the middle fingertip to the distal crease of the wrist 0.192 ± 0.005 m) served as subjects. The subjects had no previous history of neuropathies or trauma to the upper limbs. All subjects gave informed consent according to the procedures approved by the Compliance Office of The Pennsylvania State University.

2.2 Apparatus

Four uni-directional piezoelectric sensors (Model 208A03, Pizeotronic) were used for force measurement. The sensors were mounted on a steel frame (140 mm × 90 mm). Steel plates (20 mm × 25 mm) were affixed to the sensors to provide finger contact areas. Cotton tapes were attached to the upper surface of the plates to increase friction and prevent the influence of finger skin temperature on the measurements. Sensors were distributed 30 mm apart in the adduction-abduction direction of the fingers. The position of the sensors could be adjusted in a range of 60 mm in the longitudinal direction of the finger to fit an individual subject's anatomy.

A wooden board was made to support and stabilize the forearm and wrist to secure a constant configuration of the posture. The surface of the sensors, the support of the wrist, and the forearm were aligned in the same horizontal plane. The left hand was naturally resting on the thigh. Force signals from the sensors were connected to separate AC/DC conditioners (M482M66, Pizeotronic). A 12-bit analog-digital convector was used for digitizing analog output. A PC 486 microcomputer was utilized for control, acquisition, and processing. See Fig. 1 for a schematic illustration of the experimental setup.

2.3 Procedure

During testing, the subject was seated in a chair facing the testing table with his upper arm at approximately 45° of abduction in the frontal plane and 45° of flexion in the sagittal plane, and the elbow at approximately 45° of flexion (Fig. 1).

Subjects were told to press maximally with various combinations of the four fingers: the index (I), middle (M), ring (R), and little (L) fingers. All 15 combinations were utilized. They are I, M, R, L, IM, IR, IL, MR, ML, RL, IMR, IML, IRL, MRL, and IMRL, respectively. For each combination, subjects were instructed to keep the uninvolved fingers on the sensors, but no attention was paid to these fingers during pressing. It was emphasized that subjects should not try to lift the uninvolved fingers in any circumstances. In case the subjects felt the uninvolved fingers were unconsciously producing forces, they were instructed to let them to do so. The subjects were given several practice trials before testing. At the beginning of each trial prior to the force production of the fingers, the program automatically adjusted the initial value of the sensor signals to zero.

The order of the 15 combinations was randomized. Two consecutive trials were performed for each finger combination. The total duration of a trial was approximately 5 s, with a period of about 2 s required for the maximum force production. The second of the two trials was used in the analysis. Breaks of 30 s were given after each trial to avoid fatigue. During the rest period, the subjects were allowed to take the fingers off the sensors and relax the muscles.

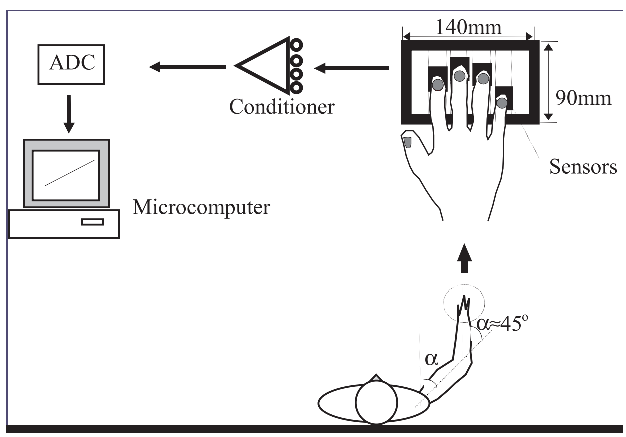

Fig. 1. Schematic drawing of the experimental setup

2.4 Data processing and statistical analysis

The digital signals were converted into force values and digitally low-pass filtered at 10 Hz with a second-order Butterworth filter. The forces of individual fingers at the instant of maximal total force production were measured for further analysis.

To characterize the interaction effects among the fingers, a nonlinear regression model of the second order was employed

$$F_{i,j} = \sum_{m=1}^{4} A_{im} X_{m,j} + \sum_{m=1}^{4}\sum_{l=1}^{4} B_{ilm} X_{i,j} X_{m,j} \quad (1)$$

where i, l, m = 1, 2, 3, 4 stand for individual fingers; i is the finger whose force is being determined; fingers 1, 2, 3, 4 correspond to I, M, R, L, respectively; j stands for one of the 15 finger combinations (I, M, R, L, IM, …, IMRL), $F_{i,j}$ is the force of finger i in a finger combination j, $X_{ij} = U_{ij}/\sum U_{ij}$; $U_{ij} = 1$ if the finger i is involved in finger combination j; and $U_{ij} = 0$ if the finger i is not involved in the combination j; and A and B are regression coefficients.

In (1), the first term is linear and the second is a nonlinear quadratic form. The quadratic form reflects the interaction among the fingers. Equation (1) can be written as a matrix expression, the product of the matrix of regression coefficients by the vector of input signals:

$$\begin{pmatrix} F_{1,j} \\ F_{2,j} \\ F_{3,j} \\ F_{4,j} \end{pmatrix} = \begin{bmatrix} A_{11} & A_{12} & A_{13} & A_{14} & B_{112} & B_{113} & B_{114} & B_{123} & B_{124} & B_{134} \\ A_{21} & A_{22} & A_{23} & A_{24} & B_{212} & B_{213} & B_{214} & B_{223} & B_{224} & B_{234} \\ A_{31} & A_{32} & A_{33} & A_{34} & B_{312} & B_{313} & B_{314} & B_{323} & B_{324} & B_{334} \\ A_{41} & A_{42} & A_{43} & A_{44} & B_{412} & B_{413} & B_{414} & B_{423} & B_{424} & B_{434} \end{bmatrix} \times \begin{pmatrix} X_{1,j} \\ X_{2,j} \\ X_{3,j} \\ X_{4,j} \\ X_{1,j}X_{2,j} \\ X_{1,j}X_{3,j} \\ X_{1,j}X_{4,j} \\ X_{2,j}X_{3,j} \\ X_{2,j}X_{4,j} \\ X_{3,j}X_{4,j} \end{pmatrix} \quad (2)$$

The statistical significance of these terms was estimated in the following way (Neter et al. 1990). When only the linear term is included, the error sum of squares is SSE(1). When both the linear and quadratic terms are included, the error sum of squares is SSE(2). If SSE(2) is smaller than SSE(1) the reduction of SSE is the result of adding the quadratic term to the regression model. To test the significance of the contribution of the quadratic term, the percentage reduction of SSE was calculated as

$$\text{Reduction (\%)} = \frac{\text{SSE (1)} - \text{SSE (2)}}{\text{SSE (1)}} \times 100\% \quad (3)$$

To estimate the magnitude of the enslaving effects, the force produced by an uninvolved finger was expressed as a percent of the maximal force produced by this finger in a single-finger task. Two-tailed Student's t-tests were used for comparison.

3 Results

Table 1 shows the individual finger forces at the instant of maximum total force production in various finger combinations. The pattern of finger forces is rather complex. However, several reproducible phenomena can be identified. In particular, the finger forces in multi-finger tasks were always smaller than the forces in the single-finger tasks (Ohstuki 1981; Kinoshita et al. 1995; Li et al. 1998a,b). Within this study we will concentrate on the interaction among the fingers and on the enslaving effects.

Interaction among the fingers. The regression coefficients of Eq. (2) are presented in Table 2. The nonlinear regression model predicted the experimental results quite accurately (Table 2). The root mean square difference was 1.22 N.

Table 3 shows that the interaction effects were very large. The drastic reduction of the SSE was observed after the nonlinear, quadratic term was added. In other words, the force of one of the fingers significantly influenced the magnitude of the force produced by the other fingers.

Enslaving. In all single-, two-, and three-finger tasks the uninvolved (slave) fingers produced a certain force.

Table 1. Force of individual fingers at the instant of maximum total force production in various tasks (newtons, mean ± SD, 10 subjects)

Task	Index	Middle	Ring	Small	Total force
I	49.1 ± 9.5	10.5 ± 6.1	5.5 ± 4.1	2.7 ± 2.4	67.8 ± 17.2
M	14.0 ± 7.0	38.0 ± 6.4	12.9 ± 7.1	4.1 ± 3.7	69.0 ± 18.2
R	9.4 ± 11.2	16.5 ± 6.5	29.9 ± 7.9	10.6 ± 5.1	66.4 ± 21.4
L	7.7 ± 6.9	6.7 ± 5.4	15.0 ± 6.1	24.8 ± 3.8	54.2 ± 17.7
IM	43.3 ± 8.9	30.3 ± 7.4	7.5 ± 5.2	2.9 ± 2.5	84.0 ± 19.0
IR	37.0 ± 10.6	14.5 ± 5.0	21.6 ± 5.5	9.2 ± 6.2	82.3 ± 19.5
IL	37.9 ± 7.9	8.1 ± 3.8	10.4 ± 4.2	18.6 ± 3.9	75.0 ± 15.9
MR	10.4 ± 7.3	37.0 ± 10.5	27.9 ± 8.8	7.7 ± 4.5	83.0 ± 20.1
ML	11.7 ± 7.4	30.4 ± 9.1	15.5 ± 7.5	16.7 ± 5.5	74.3 ± 21.0
RL	9.9 ± 8.6	19.6 ± 8.4	28.5 ± 9.0	19.6 ± 7.8	77.6 ± 19.7
IMR	34.1 ± 10.3	32.4 ± 6.8	20.0 ± 5.1	5.1 ± 4.6	91.6 ± 21.3
IML	34.8 ± 10.2	20.7 ± 5.6	11.2 ± 7.9	15.8 ± 6.9	82.5 ± 20.8
IRL	35.5 ± 10.1	10.2 ± 5.2	19.8 ± 7.1	18.0 ± 5.3	83.5 ± 20.8
MRL	11.6 ± 6.3	28.6 ± 11.2	27.7 ± 8.0	18.1 ± 5.4	86.0 ± 22.1
IMRL	32.4 ± 6.6	26.5 ± 8.1	22.1 ± 6.4	16.1 ± 7.6	97.1 ± 22.3

Interaction among the fingers. The regression coefficients of Eq. (2) are presented in Table 2. The nonlinear regression model predicted the experimental results quite accurately (Table 2). The root mean square difference was 1.22 N

Table 2. Regression coefficients

Finger i	A_{i1}	A_{i2}	A_{i3}	A_{i4}
(a) Linear term				
1 (I)	48.1	−37.9	−50.4	−116.8
2 (M)	−13.4	35.8	−16.3	−13.8
3 (R)	0.9	−7.0	48.9	49.9
4 (L)	−0.1	6.5	−15.6	65.3

Finger i	B_{i11}	B_{i12}	B_{i13}	B_{i14}	B_{i22}	B_{i23}	B_{i24}	B_{i33}	B_{i34}	B_{i44}
(b) Quadratic (interaction) terms										
1 (I)	0.4	103.9	100.8	171.9	51.6	109.7	182.5	59.2	197.4	124.0
2 (M)	24.1	52.4	61.4	33.6	2.1	76.7	48.1	32.9	77.2	21.1
3 (R)	4.6	18.7	0.1	−30.8	19.7	30.7	−4.9	−19.1	−28.0	−35.0
4 (L)	2.7	−0.9	38.4	−13.7	−2.7	26.7	−27.0	26.1	−1.3	−41.1

The EE were (A) large, (B) nearly symmetrical, (C) larger for the neighboring fingers, and (D) non-additive (see Table 4).

A. Uninvolved fingers can produce a force as large as 54.7% of their maximum in single-finger tasks (Table 4, the data for the ring finger when the middle and little finger produced maximal force).

B. The influence of finger A on finger B was approximately of the same magnitude as the influence of finger B on finger A (Fig. 2). For example, when the middle/ring finger is maximally active the force of the ring/middle finger equaled 43.1/43.4% of the corresponding maximal force ($t = -0.193$, $p = 0.851$). Enslaving effects for the other finger pairs were: 27.6 and 28.5% for the index and middle fingers ($t = 0.023$, $p = 0.981$); 18.4 and 19.1% for the I and R ($t = 0.115$, $p = 0.911$); 17.6 and 16.5% for the M and L ($t = -0.350$, $p = 0.734$), 50.2 and 42.7% for the R and L ($t = -1.73$, $p = 0.118$), and 10.9 and 15.6% for the I and L ($t = 0.434$, $p = 0.352$). Hence, the effects were approximately symmetrical.

C. In the single-finger tasks, the EE were larger for the neighboring fingers. The enslaving effects produced

Table 3. The linear regression model versus the model with both linear and quadratic terms. The error sum of squares and the percent reduction.

Finger i	SSE(1)	SSE(2)	Reduction %
1 (I)	367.1	26.9	92.7
2 (M)	226.2	39.5	82.5
3 (R)	106.6	8.3	92.2
4 (L)	73.3	14.8	79.8

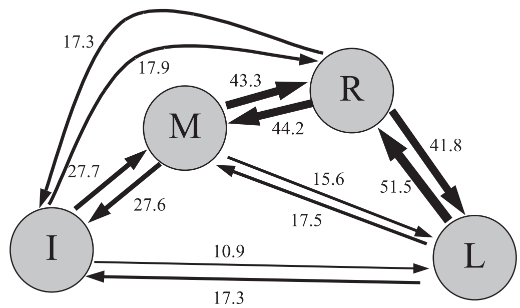

Fig. 2. Force enslaving among fingers during single-finger tasks. The arrows originated from master fingers and point at slave finger. The values besides the lines show the enslaving effects (in % of the maximal finger force). The line thickness is proportional to the magnitude of the enslaving. Note that the enslaving effects are nearly symmetrical

Table 4. Enslaving effects in the multiple-finger force production, % of the maximal force in the single finger tasks. Average data ± SD

Master fingers	Enslaved fingers			
	I	M	R	L
I	**100.0 ± 0.0**	27.7 ± 16.6	17.9 ± 12.8	10.9 ± 8.9
M	27.6 ± 11.7	**100.0 ± 0.0**	43.0 ± 22.7	15.6 ± 12.1
R	17.3 ± 20.0	44.2 ± 16.7	**100.0 ± 0.0**	41.8 ± 18.0
L	14.6 ± 13.0	17.5 ± 14.1	51.5 ± 21.8	**100.0 ± 0.0**
IM	**88.6 ± 9.1**	**81.5 ± 21.7**	24.4 ± 15.5	11.3 ± 9.5
IR	**74.9 ± 15.6**	37.7 ± 10.4	**73.5 ± 12.2**	34.7 ± 19.6
IL	**79.3 ± 18.6**	20.9 ± 9.5	34.9 ± 11.8	**75.0 ± 9.1**
MR	21.2 ± 15.0	**97.3 ± 22.2**	**94.0 ± 17.4**	31.5 ± 19.4
ML	23.3 ± 12.9	**81.7 ± 24.3**	54.7 ± 29.1	**67.3 ± 19.2**
RL	14.1 ± 11.4	46.8 ± 19.8	**97.6 ± 11.9**	**87.3 ± 7.8**
IMR	**69.0 ± 13.8**	**86.5 ± 16.0**	**68.4 ± 15.6**	20.8 ± 18.7
IML	**71.8 ± 17.6**	**57.7 ± 23.9**	36.1 ± 17.6	**61.9 ± 20.7**
IRL	**72.5 ± 15.5**	27.7 ± 14.3	**65.7 ± 13.3**	**71.8 ± 13.7**
MRL	23.8 ± 12.1	**75.3 ± 25.9**	**92.7 ± 14.1**	**72.1 ± 14.9**
IMRL	**67.1 ± 12.8**	**71.3 ± 21.5**	**74.9 ± 14.0**	**63.8 ± 25.7**

Note: boldfaced are the percentages that are *not* due to the enslaving effects

Table 5. Non-additivity and occlusion of EE. Enslaving force in two- and three-finger tasks as a % of the maximal EE in a one-finger task

Slave finger	Two-finger tasks						Three-finger tasks
	IR	II	MR	ML	RL	IM	
I			0.77	0.84	0.51		0.86
M	0.85	0.47			1.06		0.63
R		0.68		1.06		0.47	0.70
L	0.81		0.75			0.72	0.48

by the index fingers were 27.7%, 17.9%, and 10.9% for the M, R, and L fingers, respectively. The enslaving effects generated by the little finger were 51.5%, 17.5%, and 14.6% for the R, M, and I fingers. The more distant the fingers, the smaller the enslaving effects.

D. The EE were non-additive. In two- and three-finger tasks the magnitude of the EE was always smaller than the sum of individual effects from the same set of fingers (Table 5). Even more, in a majority of cases the EE from two and three fingers was smaller than the effect from just one finger. We coined this phenomenon *occlusion*. For instance, in the IM task the ring finger was activated to the level of 24.4% of its maximal force. In the M tasks the level of activation was 43.0%. The same is true for other fingers and tasks. The occlusion was *not* observed in only two cases: (a) the R finger in the ML task and (b) the M finger in the RL task. The occlusion was always recorded in the three-finger tasks. The EE for the three-finger combinations were constantly smaller than at least in one of the single-finger tasks and one of the two-finger tasks.

An illustrative example of the force-force relationships in individual attempts is presented in Fig. 3. With the exception of the little finger in the I and M tasks, the enslaving force started to increase with the first rise of the master force level. There is no perceptible threshold. This finding suggests that the slacks in the anatomical intertendinous connections were negligible. The force-force functions were increasing (have positive derivatives) but in the majority of cases could barely be considered exactly linear.

4 Neural network modeling

Available anatomical and physiological evidence was used to construct a three-layer network with direct input-output connections, a *basic network* (Fig. 4).

4.1 Basic network

The basic network incorporated the following ideas/hypotheses:

1. Existence of two groups of muscles and muscle compartments. Each muscle/compartment of the first group serves an individual finger (uni-digit muscles) and each muscle/compartment of the second group serves several fingers (multi-digit muscles). The first group of muscles is represented in the neural network by a direct one-to-one connection from the input to

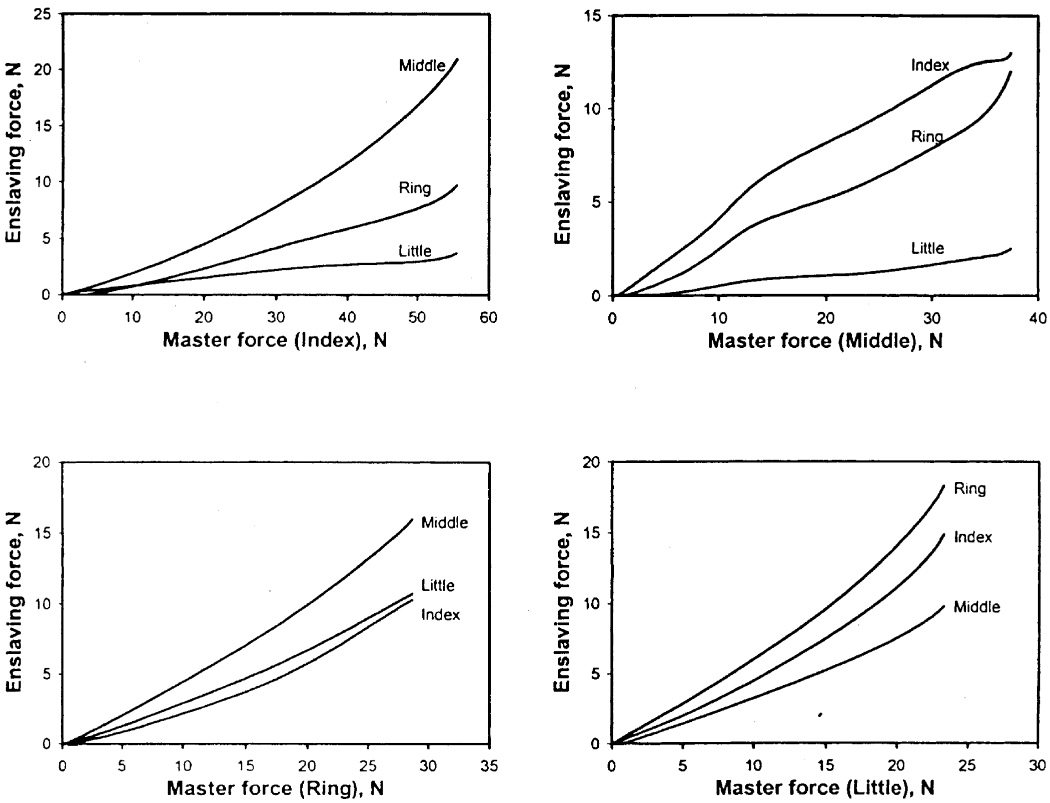

Fig. 3. Force-force curves of master finger and enslaving fingers

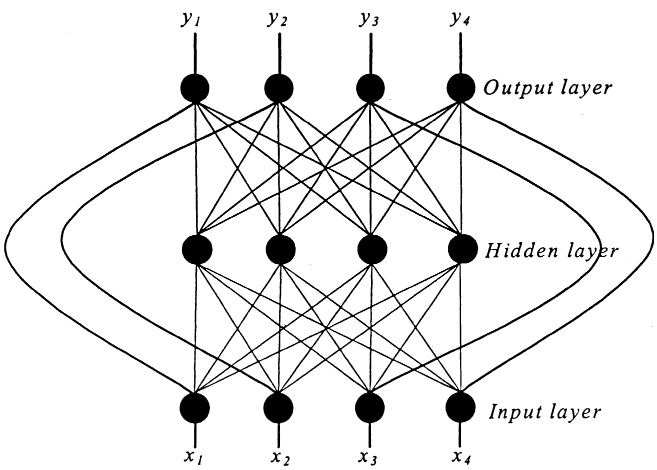

Fig. 4. Basic network. The index, middle, ring and little finger correspond to 1, 2, 3, and 4, respectively

the output layer. The second group is represented by the hidden layer and its multiple connections.
2. The 'ceiling' phenomenon was modeled by specific transfer characteristics of the hidden layer neurons: the output of the hidden layer was set as inversely proportional to the number of fingers involved. Note that in the model the 'ceiling' effects are only assigned to the multi-digit muscles of the hand.
3. The enslaving effects were modeled by the connection weights from the hidden to the output layer.

The model consists of three layers: the input layer that models a central neural drive; the hidden layer modeling extrinsic finger flexors serving several fingers simultaneously; and the output layer representing finger force output. Note the existence of direct input-output connections that model intrinsic hand muscles serving individual fingers.

4.2 Mathematical description of the network functioning

The net input to the jth unit of the hidden layer from the input layer is

$$s_j^{(1)} = \sum_{i=1}^{4} w_{ij}^{(1)} x_i \qquad j = 1,2,3,4 \tag{4}$$

where $w_{ij}^{(1)}$ are connection weights from the ith unit in the input layer to the jth unit in the hidden layer. The transfer characteristic of input/output in the hidden layer is described as

$$z_j = f_1(s_j^{(1)}) = \frac{w_{jj}^{(1)} x_j}{s_j^{(1)}} \qquad j = 1,2,3,4 \tag{5}$$

where z_j is the output from the hidden layer. The net input to the kth unit in the output layer ($s_k^{(2)}$) from the hidden layer is expressed as

$$s_k^{(2)} = \sum_{j=1}^{4} w_{jk}^{(2)} z_j + v_k x_k \qquad k = 1,2,3,4 \tag{6}$$

where $w_{jk}^{(2)}$ are connection weights from the jth unit in the hidden layer to the kth unit in the output layer. v_k are the connection weights directly from the kth unit in the input layer to the kth unit in the output layer. An identity input/output transfer relationship was defined at the output layer, i.e.,

$$y_k = f_2(s_k^{(2)}) = s_k^{(2)} \qquad k = 1,2,3,4 \tag{7}$$

The inputs to the network were set at $x_i = 1$, if finger i was involved in the task, or $x_i = 0$ otherwise. The weights from the input layer to the hidden layer were set as a unit constant ($w_{ij}^{(1)} = 1$).

4.3 Training by using backpropagation

The network was trained using a backpropagation algorithm (Bose and Liang 1996). Let the training exemplar set be $\{\vec{x}(l), \vec{d}(l)\}_{i=l}^{15}$, where
$\vec{x}(l) = [x_1(l), x_2(l), x_3(l), x_4(l)]^T$ is the input pattern vector to the network and
$\vec{d}(l) = [d_1(l), d_2(l), d_3(l), d_4(l)]^T$ is the desired output vector corresponding to the input pattern $\vec{x}(l)$.

$$x_i(l) = \begin{cases} 1 & \text{if the finger is intended to produce force} \\ 0 & \text{if the finger is not intended to produce force} \end{cases}$$

where i = 1, 2, 3, 4, indicating the fingers, l = 1, 2, ..., 15, indicating the 15 finger combinations, and $\vec{d}(l)$ is the finger force output from experiment for a given finger combination task l. The sum of squares of the error over all input units of all exemplars is defined by

$$E = \sum_{i=1}^{15} \left\{ \frac{1}{2} \sum_{k}^{4} = 1 [y_k(l) - d_k(l)]^2 \right\} \tag{8}$$

The objective is to adjust the network weights ($w_{jk}^{(2)}$ and v_k, where j, k = 1, 2, 3, 4) to minimize the error function E. The gradient descent method was used to train the networks by repeatedly presenting the training exemplar set.

Since the basic network contains connections directly from the input layer to the output layer, the functions provided by commercially available software packages such as Neural Network Toolbox (Mathworks) were not applicable. We programmed the process in the environment of Matlab (Mathworks).

4.4 Results of the training

On application of the backpropagation algorithm with a set of initial weights, a satisfactory result for this problem was obtained after 500 epochs with a learning rate of 0.01. Figure 5 is a plot of root mean square (RMS) error generated in the training process as a function of epochs when the network was trained by all 15 combinations. The error serves as a measure for performance of the network. The final network values yielded a RMS error between the results of the

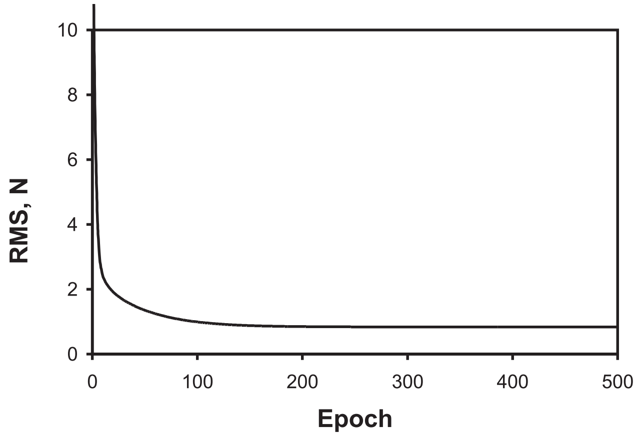

Fig. 5. The root mean square error of finger force as a function of training epochs

experiment and the network output of 1.14 N. This value is smaller than the magnitude of the standard deviation of force production for any of the individual fingers. It was concluded that the predicted finger forces closely matched the experimental data.

The following matrix of the connection weights $w^{(2)}$, also called a *connection matrix*, and the *gain* vector $[v]$ were calculated. The rows of the connection matrix, i, correspond to the outgoing signals from the hidden layer and the columns correspond to the units/fingers of the output layer, j.

$$[w^{(2)}] = \begin{bmatrix} 32.7 & 9.1 & 3.8 & 3.7 \\ 14.2 & 29.0 & 13.6 & 3.5 \\ 9.0 & 20.2 & 22.4 & 10.9 \\ 8.8 & 7.6 & 16.0 & 17.2 \end{bmatrix} \qquad [v] = \begin{bmatrix} 16.9 \\ 10.1 \\ 8.3 \\ 7.2 \end{bmatrix} \tag{9}$$

4.5 Network recall and validation

Figure 6a–c are the plots of the simulated results (open circles) generated in the recall phase and compared to the experimental results (solid circles).

The network was validated in three ways.

1. The training set included all 15 tasks. The final network values were compared with the experimentally recorded data (Fig. 6a). As already mentioned, all the predicted values of the finger forces were close to those registered in the experiments; the differences were much smaller than one standard deviation. The RMS difference was 1.14 N.
2. The training sets included only 14 tasks. The task that was not included in the training was used for validation. This procedure was repeated 15 times. The results are presented in Fig. 6b. The RMS difference for the 15 untrained finger combinations was 2.22 N. Again the predicted values were in the range of ± 1 SD.
3. Network training was performed on the four sets that did not include: (a) one-finger tasks, four tasks total; (b) two-finger tasks, six tasks total; (c) three-finger tasks, three tasks total; and (d) a four-finger task, one task. Hence, the training was performed on 11-, 9-, 12-, and 14-task sets, respectively. The finger force values for the tasks that were not used in the training sets were calculated and compared with those that were experimentally recorded. The RMS equaled 3.18 N for the one-finger tasks, 2.08 N for the two-finger task, 2.18 N for the three-finger tasks, and 0.57 N for the four-finger task. All of these tasks were not included in the training sets. The grand average RMS was 2.30 N. Again, the difference between the predicted and recorded values was in the range of ± 1 SD (Fig. 6c).

Overall, the network worked quite well.

4.6 Training of $[w^{(1)}]$ and $[w^{(2)}]$

In the basic network, the connection weights from the input layer to the middle layer, $[w^{(1)}]$, were set to units. The selection was based on the idea that when the input signal is transmitted to the middle layer it is equally shared among the involved fingers. At the next stage of analysis this assumption was removed and both layers of the network were trained by the backpropagation procedure. The connection weights were computed (Table 6). The connection weights $[w^{(2)}]$ were similar (but not exactly equal) to the connection weights of the basic model. The same is true for the gain coefficients, $[v]$. Hence, the model is robust with respect to the procedures used to estimate the connection weights.

After application of Eqs. (1) and (2) the output signals from the hidden layer were determined (Table 7). Their sum was close to 1 (in the main model it was set exactly at 1) and with few exceptions the individual output signals were close to $1/n$ (in the main model the signals were set precisely at $1/n$). The largest deviation from the values 0.5/0.5 that were assumed in the main model was observed in the RL finger combination, 0.87 and 0.19. In one-finger tasks, the sum $\sum = 1.00$.

The closeness of the sum of the output signals from the hidden layer to 1 supports the ceiling hypothesis. It appears that during maximal voluntary contraction of the fingers the central signal to the multi-digit muscles is limited in magnitude and is shared between all involved fingers. The performance of the modified model with coefficients $[w^{(1)}]$ computed from the experimental data was slightly worse than the performance of the basic model (RMS $= 1.30$). Because of the good performance of the basic model, its simplicity, and obvious operation, we prefer the basic model to its more complicated variants.

4.7 Contribution of uni-digit and multi-digit muscles (v vs. $w^{(2)}$ contribution)

The network permits estimation of the contribution of uni-digit muscles (mainly intrinsic muscles of the hand) and multi-digit muscles (mainly the extrinsic hand

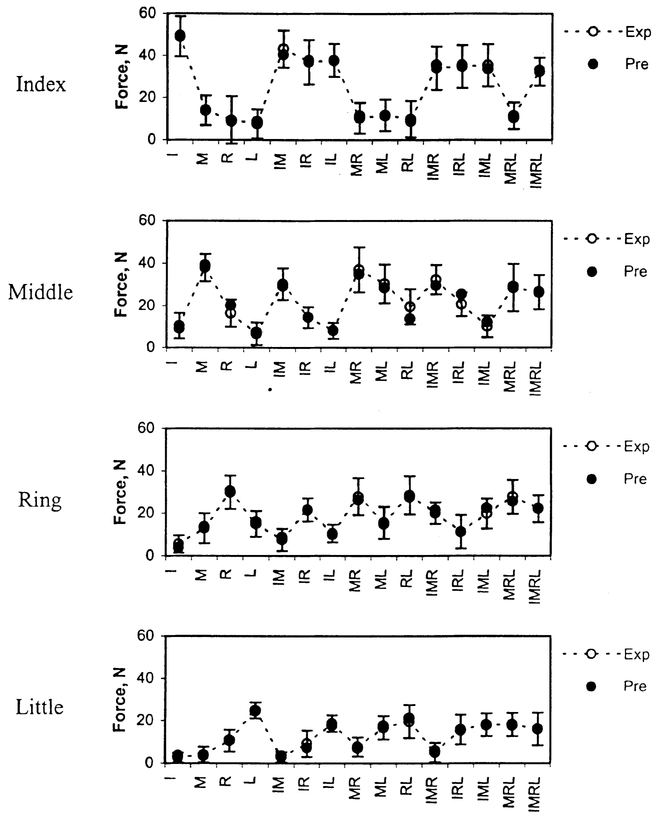

(a)

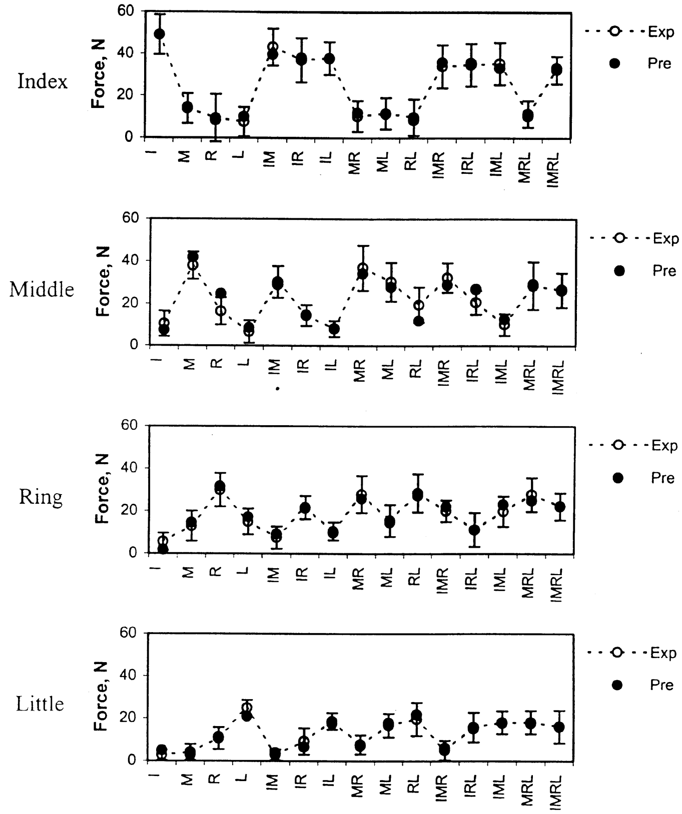

(b)

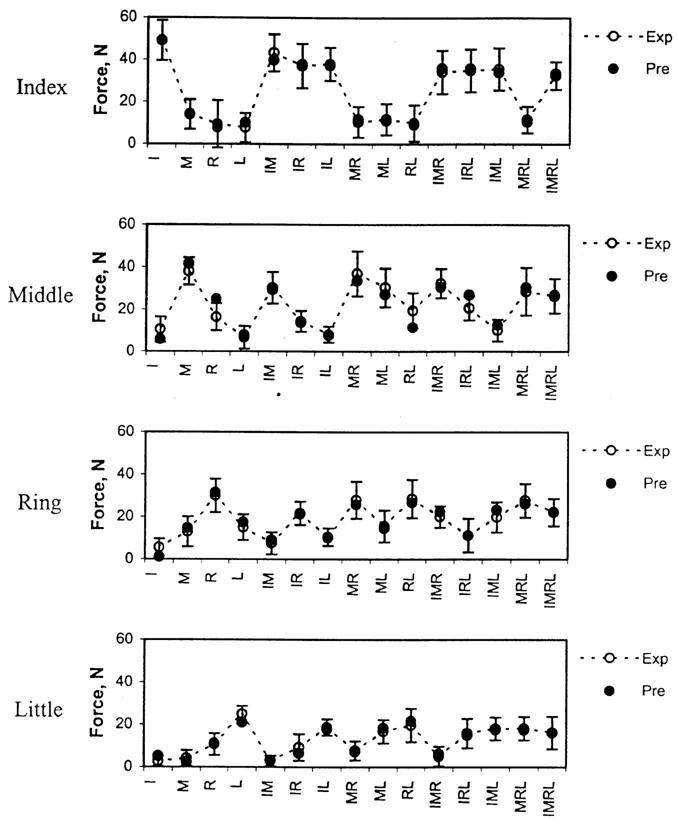

(c)

Fig. 6. Predicted vs. experimental results. The figures are for different training protocols: (a) The network was trained by all 15 combinations. (b) The network was trained 15 times using 14 combinations each time. (c) The network was trained 4 times, without 1-, 2-, 3-, 4-finger combinations respectively

Table 6. The training results of the modified model, $[w^{(1)}]$, $[w^{(2)}]$, and $[v]$

Finger	Connection weights from the input to the hidden layer, $w_{ij}^{(1)}$				Connection weights from the hidden to the output layer, $w_{ij}^{(2)}$				v_j
	1	2	3	4	1	2	3	4	
1	11.6	16.2	12.9	4.2	32.0	10.5	4.6	3.3	17.6
2	8.1	13.2	9.5	5.3	12.6	30.6	13.3	2.9	8.5
3	14.2	11.5	14.9	20.3	9.0	18.0	23.7	10.7	5.8
4	13.5	10.6	2.2	4.8	8.6	5.9	15.3	16.3	8.2

Table 7. Output of the middle layer

Finger	Task										
	IM	IR	IL	MR	ML	RL	IMR	IML	IRL	MRL	IMRL
1	0.59	0.45	0.46	0	0	0	0.34	0.35	0.29	0	0.24
2	0.45	0	0	0.54	0.56	0	0.32	0.33	0	0.37	0.26
3	0	0.53	0	0.61	0	0.87	0.40	0	0.50	0.56	0.38
4	0	0	0.53	0	0.47	0.19	0	0.33	0.16	0.16	0.14
$\sum$	1.04	0.98	0.99	1.15	1.03	1.06	1.06	1.01	0.95	1.09	1.02

Note the output from the middle layer in the four one-finger tasks was exactly 1.0

muscles) to the total force production. The results are presented in Fig 7. In different tasks, the uni-digit muscles contribute from 25% to 50% of the force produced by a given finger.

4.8 Normalized matrices

The coefficients of the connection matrix as well as the gain coefficients have the dimensionality of force; thus they are expressed in newtons per one unit of (dimensionless) command. The connection matrix cannot be

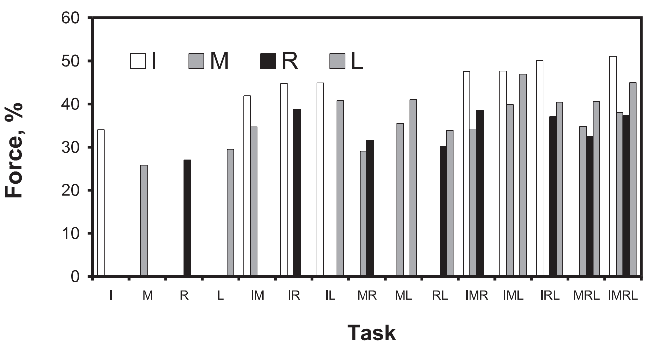

Fig. 7. Relative contribution of uni-digit (intrinsic) muscles in different tasks. The contributions of the extrinsic muscles are 100% minus the contribution of the intrinsic muscles

immediately applied to compare sharing patterns in people with different force potential, for instance in strength athletes and untrained women. To do that, two normalized matrices are suggested. The elements of the first matrix, called the *master matrix*, are normalized in rows with respect to $w_{ii}^{(2)}$, i.e.,

$$w_{ij}^{M} = \frac{w_{ij}^{(2)}}{w_{ii}^{(2)}} \times 100\% \qquad i, j = 1, 2, 3, 4 \tag{10}$$

The coefficients $w_{ij}^{(2)}$ $(i \neq j)$ characterize the force produced by the enslaved fingers as a percentage of the master finger force.

The elements of the second matrix, called the *enslaving matrix*, are normalized with respect to $w_{jj}^{(2)}$, that is, the normalization is done in columns. They characterize the potential level of enslaving of a given finger.

$$w_{ij}^{E} = \frac{w_{ij}^{(2)}}{w_{jj}^{(2)}} \times 100\% \qquad i, j = 1, 2, 3, 4 \tag{11}$$

For instance, the index finger can be enslaved up to a level of 43.4% of its direct activation by the activation of the middle finger, 27.5% by the ring finger, and 26.9% by the little finger.

The master matrix and enslaving matrix are listed in Table 8.

Table 8. The master matrix and enslaving matrix (%)

	Master matrix, % master finger force				Enslaving matrix, % same finger maximal force			
	1	2	3	4	1	2	3	4
1	100.0	27.8	11.6	11.3	100.0	31.4	17.0	21.5
2	49.0	100.0	46.9	12.1	43.4	100.0	60.7	20.3
3	40.2	90.2	100.0	48.7	27.5	69.7	100.0	63.4
4	51.2	44.2	93.0	100.0	26.9	26.2	71.4	100.0

5 Discussion

5.1 Finger interaction

Interdependent action of fingers has been an object of both anatomical (Fahrer 1981) and neurophysiological (Schieber 1991) research. In particular, studies of finger kinematics have shown that voluntary extension/flexion of one finger can induce accompanying involuntary flexion/extension of other fingers. Interaction effects, in particular enslaving, are a quantitative outcome/measure of the combined action of several factors.

The following mechanisms might have contributed to the interaction/enslaving effects: (a) peripheral mechanical coupling, (b) multi-digit motor units in the extrinsic flexor and extensor muscles, and (c) diverging central commands. At a peripheral level, enslaving can be explained by the multiple mechanical connections between the tendons (juncturae tendinum) and muscle compartments of m. flexor digitorum superficialis and flexor digitorum profundus that act on all four fingers (Fahrer 1981; Schroeder et al. 1990; Leijnse et al. 1993; Leijnse 1997). In a recent paper, Leijnse (1997) presented a biomechanical model of anatomical and functional interconnections between two deep flexor tendons. Though mechanical coupling between the tendons of the extrinsic finger flexors in the forearm seems to be certain (see, for instance, Fahrer 1981; Kilbreath and Gandevia 1994; Leijnse 1997), the contribution from these mechanical connections during isometric tasks is not evident. This is especially true for non-adjacent fingers, such as the index finger and the little finger. The discovered phenomenon of the EE occlusion can barely be explained only by the mechanical interconnections among muscles and tendons and suggests a substantial contribution of neural factors into the EE. Existence of co-activation was confirmed by the experiments on a hand in which all intertendinous connections were surgically removed (Leijnse 1997).

Some motor units of the extrinsic flexor and extensor muscles may have insertion to the tendons of different digits. Multi-digit motor units as well as single-digit units have been found in the forearm muscles of monkeys (Eccles et al. 1968). However, when compared with humans, monkeys have less 'dexterity', i.e. lower ability to move fingers independently (Kimura and Vandewolf 1970). The proportion of the multi- and single-digit motor units in the extrinsic muscles serving human fingers remains unknown. For instance, Kilbreath and Gandevia (1994) reported that when subjects lifted weights exceeding 2.5% MVC with one finger, portions of m. flexor digitorium profundus serving other fingers were also active. In the cerebral cortex, the representations of different fingers in the primary motor cortex overlap extensively. This has been shown in both single neuron studies in monkeys (Schieber and Hibbard 1993) and blood flow measurements in humans (Sanes et al. 1995). Lejinse (1997), studying a patient with surgically removed passive connections between all deep flexor tendons, found that the master and enslaving forces were strictly proportional. In this subject, the EE can only result from co-activation or from passive connections between the muscle bellies.

Hence, our data agreed with the postulate that the inter-finger force transfer is caused by several factors.

5.2 Neural network modeling

According to Iberall and Fagg (1996, p. 244) hand function is 'an ideal candidate for using neural networks'. However, until now, the grasping – the number of fingers, selecting the opposition, and selecting, a hand opening size – has only been modeled by the neural networks (Iberall et al. 1989; Uno et al. 1993; Iberall and Fagg 1996). This study concentrates on other aspects of hand and finger motion.

The neural network is based on the following two ideas. (1) A central neural drive is delivered to the two groups of muscles: (a) single-digit muscles, mainly intrinsic muscles of the hand (this neural drive is not shared among the muscles/fingers) and (b) multi-digit muscles, mainly extrinsic muscles in the forearm. (2) The drive to the multi-digit muscles is shared among specific muscle compartments serving singular digits.

5.2.1 How does the net work? One of the advantages of the developed network is its simplicity. Owing to the uncomplicated structure of the network, the limited assortment of neurons, and a restricted number of postulations, the network machinery is easy to understand and describe as a matrix equation.

$$\begin{pmatrix} F_1 \\ F_2 \\ F_3 \\ F_4 \end{pmatrix} = \frac{1}{n} \begin{bmatrix} w_{11}^{(2)} & w_{11}^{(2)} & w_{11}^{(2)} & w_{11}^{(2)} \\ w_{11}^{(2)} & w_{11}^{(2)} & w_{11}^{(2)} & w_{11}^{(2)} \\ w_{11}^{(2)} & w_{11}^{(2)} & w_{11}^{(2)} & w_{11}^{(2)} \\ w_{11}^{(2)} & w_{11}^{(2)} & w_{11}^{(2)} & w_{11}^{(2)} \end{bmatrix} \bullet \begin{pmatrix} x_1 \\ x_2 \\ x_3 \\ x_4 \end{pmatrix} + \begin{pmatrix} v_1 & 0 & 0 & 0 \\ 0 & v_2 & 0 & 0 \\ 0 & 0 & v_3 & 0 \\ 0 & 0 & 0 & v_4 \end{pmatrix} \bullet \begin{pmatrix} x_1 \\ x_2 \\ x_3 \\ x_4 \end{pmatrix} \quad (12)$$

where n is the number of fingers involved in the task.

As an example, consider the activity of the middle finger in the one- and two-finger tasks. Based on the model, in the one-finger task the one-digit muscles should contribute 10.1 N and the multi-digit muscles 29.0 N (in total 39.1 N; the experimental value was 38.0 N). In the two-finger task with the index and middle fingers active, the contribution of the one-digit muscles is the same as previously, 10.1 N; the contribution from the multi-digit muscles is $0.5 \times (29.0 + 9.1) = 19.1$ N. In total, the predicted force should be 29.2 N. The real force was 30.3 N.

According to a hypothesis suggested by Ohtsuki (1981), the force deficit is a result of ipsilateral synergistic inhibition: activation of one finger inhibits activity of its adjacent fingers. In general, the existence of synergistic inhibition in the neuromotor system – as opposed to reciprocal inhibition – has not been confirmed in the literature. The network model accounts for the force deficit as well as for sharing and enslaving. According to the model, all the three phenomena are a consequence of the existence of the uni- and multi-digit muscles.

5.2.2 Comparing with minimal norm optimization. The optimization approach has been broadly used to explore the sharing/motor redundancy problem at the level of individual muscles and their contribution to a total joint torque (for the latest reviews, see Bogert 1994; Herzog 1996). However, because individual muscle forces cannot be measured immediately, the optimization results cannot be directly validated. It seems natural to employ an optimization method for the finger force sharing where all the finger forces can be directly measured. Various optimization techniques and cost functions have been used in the literature to examine how individual muscles contribute to the resultant moment at a joint. For instance, in the review paper by Zatsiorsky and Prilutsky (1992), 26 different cost functions are analyzed.

In this study, the optimization is based on the presumption that the CNS is trying to minimize a certain norm of the relative force values (% of F_{mi}). More formally, the problem can be formulated as follows:

Minimize

$$g(F_i) = \left(\sum_i^n \left(\frac{F_i}{F_{mi}}\right)^p\right)^{\frac{1}{p}} \quad (13)$$

Subject to constraint function:

$$h(F_i) = \sum_{i=1}^n F_i = F_{\text{tot}} \quad (14)$$

where i stands for a finger involved in a task, F_i are individual finger forces, p is value of power ($p > 1$), and n is the number of fingers involved in the tasks ($n = 2, 3, 4$). F_{tot} is the total force level achieved by all the involved fingers. The model can be stated as follows: find the force-sharing pattern by minimizing a certain norm of relative force. To solve the problem we used the method of Lagrange multipliers and, as a result, arrived at the following forces of the individual fingers.

$$F_i = F_{\text{tot}} \frac{(F_{mi})^{\frac{p}{p-1}}}{\sum_{k=1}^n (F_{mk})^{\frac{p}{p-1}}} \quad (15)$$

Figure 8 reflects the accuracy of finger force prediction by optimizing the cost function – the norm of relative force – while changing values of the power ($1 < p < 100$). Three tasks, IM, IMR, and IMRL, were chosen as examples. Generally, when an appropriate power value was chosen the model predicted the force sharing among fingers quite well. For the IM task the best prediction occurred at $p = 3.5$, at which the RMS error was 0.02 N. For the IMR and IMRL tasks, the larger the p, the smaller the errors. The RMS errors at $p = 100$ for the IMR and IMRL tasks were 1.76 N and 0.58 N, respectively.

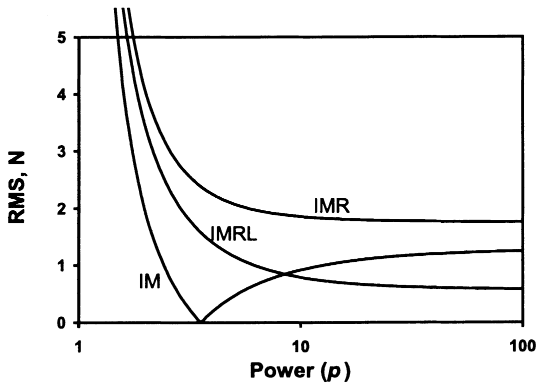

Fig. 8. The root mean square error of finger force as a function of the power of the minimal norm cost function. The x axis is scaled in logarithmic unit

As compared with neural network modeling, the optimization approach seems to be less efficient for the following reasons:

1. Only force sharing is modeled. The method does not address the force deficit and enslaving.
2. A different motor task requires a separate optimization procedure.
3. The parameters of the cost function do not have a simple anatomical or physiological meaning. They are just mathematical abstractions. For instance, why is the optimal power value in the IM task equal to 3.5? The similarity of the experimental and predicted results does not imply that the ways of solving the problem are also similar. The CNS is evidently using other ways – not the cost function minimization – to solve the redundancy problem.

5.2.3 What does the network really model? The suggested network portrays a transformation of the central neural command into finger force values. If there were no interaction and interconnection among fingers, the command, 0 or 1, would transform into finger forces in a straightforward manner. Mathematically, the command should simply be multiplied by gain coefficients. However, both the anatomical facts, specifically the existence of extrinsic muscles with multiple tendons to the individual fingers (Schieber 1991; Schroeder et al. 1990; Kilbreath and Gandevia 1994), and the experimental phenomena, specifically force deficit and enslaving, do not permit us to accept the straightforward relationship between the voluntary command to an individual finger and the level of the force produced by this finger.

The implicit idea behind the suggested network is that all the three reported phenomena – sharing pattern, force deficit, and enslaving – are a consequence of the interconnections among the fingers. These interconnections are both peripheral (on the muscle-tendon level) and central (on the level of the CNS). The central interconnections result in conjoint activation of the compartments of the extrinsic muscles serving different fingers.

If the network adequately represents reality, it means that there is no direct correspondence/proportionality between the 'intensity' of the neural command to an individual finger (whatever this 'intensity' is and without regard to how the 'intensity' is measured) and the finger force. This conclusion is in a good agreement with the data of Schieber (1991) obtained on monkeys. In multi-finger tasks, to produce a given finger force it is not enough to send a properly scaled command to the muscles serving the finger; the commands to other fingers should also be assessed and controlled.

Acknowledgements. The study was partly supported by grants HD-30128 and NS-35032 from the National Institutes of Health, and a research fund from the College of Health and Human Development, The Pennsylvania State University. The comments suggested by Robert Gregory and Mathew Pain are appreciated.

References

Bernstein NA (1967) The co-ordination and regulation of movements. Pergamon Press, Oxford

Bogert AJ van den (1994) Analysis and simulation of mechanical loads on the human musculoskeletal system: a methodological overview. Exerc Sport Sci Rev 22:23–51

Bose NK, Liang P (1996) Neural network fundamentals with graphs, algorithms, and applications. McGraw-Hill, New York

Brand RA, Pedersen DR, Friederich JA (1986) The sensitivity of muscle force predictions to changes in physiologic cross-sectional area. J Biomech 19:589–596

Crowninshield RD, Brand RA (1981a) A physiologically based criterion of muscle force prediction in locomotion. J Biomech 14:793–801

Crowninshield RD, Brand RA (1981b) The prediction of forces in joint structures: distribution of intersegmental resultants. Exercise Sci Rev 9:159–181

Crowninshield RD, Johnston RC, Andrews JG, Brand RA (1978) A biomechanical investigation of the human hip. J Biomech 11:75–85

Eccles RM, Phillips CC, Ghien-Ping W (1968) Motor innervation, motor unit organization and afferent innervation of m. extensor digitorum communis of the baboon's forearm. J Physiol (Lond) 198:179–192

Fahrer M (1981) Interdependent and independent actions of the fingers. In: Tubiana R (ed) The hand. Saunders, Philadelphia, pp 399–401

Herzog W (1996) Force-sharing among synergistic muscles: theoretical considerations and experimental approaches. Exerc Sport Sci Rev 24:173–201

Howard JD, Enoka RM (1991) Maximum bilateral contractions are modified by neurally mediated interlimb effects. J Appl Physiol 70:306–316

Iberall T, Fagg AH (1996) Neural network models for selecting hand shapes. In: Wing AM, Haggard P, Flanagan JR (eds) Hand and brain. Academic Press, San Diego pp 243–264

Iberall T, Preti MJ, Zemke R (1989) Task influence on timing and grasp patterns in human prehension. Soc Neurosci Abstr 15:397

Kilbreath SL, Gandevia SC (1994) Limited independent flexion of the thumb and fingers in human subjects. J Physiol (Lond) 479:487–497

Kimura D, Vanderwolf CH (1970) The relation between hand preference and the performance of individual finger movements by left and right hands. Brain 93:769–774

Kuo AD (1994) A mechanical analysis of force distribution between redundant, multiple degree-of-freedom actuators in the humans: implications for the central nervous system. Hum Movement Sci 13:635–663

Latash ML (1996) How does our brain make its choices? In: Latash ML, Turvey MT (eds) Dexterity and its development. Erlbaum, Mahwah, NJ, pp 277–304

Leijnse JNAL (1997) Measuring force transfers in the deep flexors of the musician's hand: theoretical analysis, clinical examples. J Biomech 30:873–882

Leijnse JNAL, Snijders CJ, Bonte JE, Landsmeer JMF, Kalker JJ, Van Der Meulen JC, Sonneveld GJ, Hovius SER (1993) The hand of the musician: the kinematics of the bidigital finger system with anatomical restrictions. J Biomech 26:1169–1179

Li ZM, Latash ML, Zatsiorsky VM (1998a) Force sharing among fingers as a model of the redundancy problem. Exp Brain Res (in press)

Li ZM, Latash ML, Zatsiorsky VM (1998b) Motor redundancy during maximal voluntary contraction in four-finger tasks. Exp Brain Res (in press)

Neter J, Wassserman W, Kutner MH (1990) Applied linear statistical models. Irwin, Butt Ridge, Ill

Ohtsuki T (1981) Inhibition of individual fingers during grip strength exertion. Ergonomics 24:21–36

Prilutsky BI, Zatsiorsky VM (1994) Tendon action of two-joint muscles: transfer of mechanical energy between joints during jumping, landing, and running. J Biomech 27:25–34

Prilutsky BI, Petrova LN, Raitsin LM (1996) Comparison of mechanical energy expenditure of joint moments and muscle forces during human movement. J Biomech 29:405–416

Rosenbaum DA, Engelbrecht SE, Bushe MM, Loukopoulos LD (1993) Knowledge model for selecting and producing reaching movements. J Motor Behav 25:217–227

Sanes JN, Donoghue JP, Thangaraj V, Edelman RR, Warach S (1995) Shared neural substrates controlling hand movements in human motor cortex. Science 268:1775–1777

Schantz PG, Moritani T, Karlson E, Johansson E, Lundh A (1989) Maximal voluntary force of bilateral and unilateral leg extension. Acta Physiol Scand 136:185–192

Schieber MH (1991) Individuated movements of rhesus monkeys: means of quantifying the independence of digits. J Neurophysiol 65:1381–1391

Schieber MH, Hibbard LS (1993) How somatotopic is the motor cortex hand area. Science 261:489–492

Schroeder HP von, Botte MJ, Gellman H (1990) Anatomy of the juncturae tendinum of the hand. J Hand Surg Am 15:595–602

Uno Y, Fukumara N, Suzuki R, Kawato M (1993) Integration of visual and somatosensory information for preshaping hand in graping movements. Adv Neural Inf Process Syst 5:311–318

Zatsiorsky VM, Prilutsky BI (1992) Estimating muscle forces from a given movement. In: Zatsiorsky VM (ed) Biomechanics of muscles and the structure of movement. Contemporary problems of biomechanics, vol 7. Russian Academy of Science, Nizhny Novgorod, pp 81–123